DOA OUTLIER MITIGATION FOR GENERALISED SPATIAL SMOOTHING

*Yuri I. Abramovich** and *Nicholas K. Spencer*
Cooperative Research Centre for Sensor Signal and Information Processing (CSSIP),
SPRI Building, Technology Park, Mawson Lakes, South Australia, 5095, Australia
yuri@cssip.edu.au nspencer@cssip.edu.au

ABSTRACT

This paper considers the problem of DOA (direction-of-arrival) estimation for a small number of fully correlated sources. The standard spatial smoothing technique [1] may be applied to this single-snapshot model, but only for a uniformly-spaced linear antenna array (ULA). In [2], we introduced a special class of nonuniform array geometry with embedded *partial arrays* and a corresponding generalised spatial smoothing (GSS) algorithm. The initialisation stage of GSS (which is followed by a local maximum-likelihood refinement) involves spatial averaging over all suitable noncontiguous sub-arrays with identical inter-sensor separations. These partial arrays are themselves nonuniform in geometry, and have a small number of sensors. It is well known that MUSIC may fail to resolve poorly-separated sources when the SNR and number of spatial averagings are insufficient, due to abnormal DOA estimates ("outliers"). An additional outlier mechanism for partial-array MUSIC occurs because each partial array has some associated *manifold ambiguity* [3, 4]. Thus for spatial smoothing, the set of (initial) DOA estimates often contains outliers. This paper introduces an algorithm which aims to identify each outlier and to correct it, if possible.

1 PARTIAL-ARRAY MUSIC (PA-MUSIC) TECHNIQUE FOR GSS

Consider the problem of DOA estimation for m fully correlated sources given an M-element ($m \ll M$) nonuniform linear array (NLA) which belongs to the special class of geometry with embedded partial arrays, introduced in [2, 5]. There we defined a *partial array* to be a group of nonuniform linear noncontiguous sub-arrays of identical co-sequence structure, where *co-sequence* simply means the sequence of consecutive inter-sensor separations (*ie.* differences).

An example geometry which belongs to this class of *embedded partial nonuniform linear array* (EPNLA) is the 7-element array

$$\boldsymbol{d}_{eg} = [0,\ 1,\ 5,\ 6,\ 9,\ 11,\ 12] \tag{1}$$

*This study was partly supported by the INTAS SASPARC grant.

where sensor positions are measured in half-wavelength units. This EPNLA has $n = 8$ embedded partial arrays, one of which is the partial array defined by the co-sequence structure

$$\boldsymbol{c}_1 = [1,\ 5] \tag{2}$$

since this co-sequence repeatedly occurs as a fixed sub-array pattern of the $\boldsymbol{d}_{eg}$ elements as follows:

$$\begin{aligned} \boldsymbol{d}_{11} &= [0,\ 1,\ 6] \\ \boldsymbol{d}_{12} &= [5,\ 6,\ 11] \\ \boldsymbol{d}_{13} &= [0,\ 5,\ 6] \\ \boldsymbol{d}_{14} &= [6,\ 11,\ 12]. \end{aligned} \tag{3}$$

Note that the instances $\boldsymbol{d}_{13}$ and $\boldsymbol{d}_{14}$ exist as mirror-images (the co-sequence order is reversed). Associated with each partial array are its *multiplicity* κ (number of occurrences or *instances*), *order* ℓ (number of co-sequence elements involved), and aperture a.

Here we illustrate DOA estimation performance using the 16-element EPNLA presented in [2, 5]:

$$\boldsymbol{d}_{55} = [0, 1, 5, 6, 8, 10, 19, 23, 26, 34, 37, 41, 44, 52, 53, 55]\,. \tag{4}$$

Table 1 shows the $\kappa\ell$-distribution and Fig. 1 illustrates the a-distribution of partial arrays for this geometry.

The GSS technique may be applied to a NLA providing it yields at least one partial array of multiplicity $\kappa \geq m$ and order $\ell \geq m$.

ℓ \ κ	3	4	5	6	7	8	9
3	33	9	0	0	0	0	0
4	32	3	0	0	0	0	0
5	12	0	0	0	0	0	0

Table 1: Partial array distribution by multiplicity (κ) and order (ℓ) for the EPNLA $\boldsymbol{d}_{55}$ for $m = 3$ and the search range $3 \leq \ell \leq 5$ and $1 \leq c \leq 18$ (see [2, 5]). There are $n = 89$ partial arrays with a total of $N = 279$ instances available for spatial smoothing.

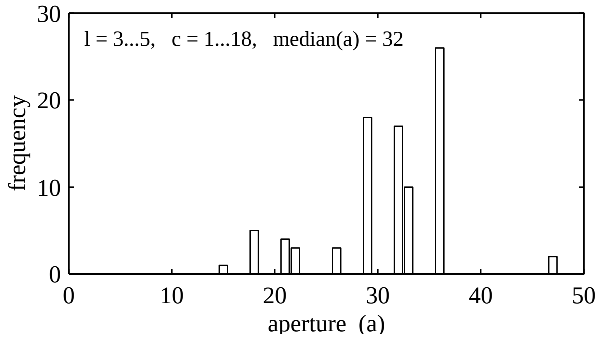

Figure 1: Aperture histogram of $\boldsymbol{d}_{55}$ partial arrays.

Let $\boldsymbol{y}_{ij}$ be the (ℓ_i+1)-variate snapshot vector corresponding to the j^{th} instance $(j = 1, \ldots, \kappa_i)$ of the i^{th} partial array $(i = 1, \ldots, n)$. If any instance of a partial array occurs as a mirror-image (*ie.* in reverse order), then the corresponding snapshot vector is observed by reversing the order of antenna samples and taking the complex conjugate of the vector. Thus for each partial array we may define the $(\ell_i+1) \times (\ell_i+1)$ partial-array covariance matrix by spatial smoothing to be

$$\hat{R}_i = \sum_{j=1}^{\kappa_i} \boldsymbol{y}_{ij}\, \boldsymbol{y}_{ij}^H. \tag{5}$$

Let $\hat{G}_i$ be the noise eigen-subspace of $\hat{R}_i$, then $\hat{G}_i$ consists of at least one eigenvector for any suitable partial array. Thus the MUSIC pseudo-spectrum for the i^{th} partial array is

$$f_i(\theta) = \left[\boldsymbol{a}_i^H(\theta)\, \hat{G}_i\, \hat{G}_i^H\, \boldsymbol{a}_i(\theta)\right]^{-1} \tag{6}$$

where $\boldsymbol{a}_i(\theta)$ is the (ℓ_i+1)-variate manifold vector corresponding to the partial array geometry. The PA-MUSIC pseudo-spectrum introduced in [2] simply involves the sum over all suitable partial arrays:

$$f_{PA}(\theta) = \sum_{i=1}^{n} \left[\boldsymbol{a}_i^H(\theta)\, \hat{G}_i\, \hat{G}_i^H\, \boldsymbol{a}_i(\theta)\right]^{-1}. \tag{7}$$

The PA-MUSIC DOA estimates, defined as the m greatest maxima of $f_{PA}(\theta)$, are then used to initialise a local maximum likelihood (ML) refinement procedure [2]. Obviously this local refinement can only be successful if these initial estimates do not contain outliers.

Unfortunately, there are two mechanisms contributing to the occurrence of abnormal DOA estimates. Firstly, since the aperture of any partial array is less than that of the original NLA, the finite number of covariance averagings (κ) and the finite signal-to-noise ratio (SNR) together mean that situations will occur where MUSIC fails to resolve poorly separated sources. This property of MUSIC occurs for scenarios crossing the threshold into the so-called *pre-asymptotic domain*, which exists for every class of array geometry [6].

The second reason is specific to partial arrays. In order to advance PA-MUSIC DOA estimation accuracy well beyond the standard M-element ULA limit, it is inevitable that the EPNLA geometry is very sparse [5, 7]. Hence there will exist a substantial number of DOA sets where the manifold vectors $\boldsymbol{a}_i(\theta)$ are linearly dependent [3, 8, 4] (*ie.* manifold ambiguities). Consequently some of the individual partial array MUSIC pseudo-spectra $f_i(\theta)$ are very likely to contain erroneous peaks. Since different partial arrays generally have different manifold ambiguity sets, we decrease the probability of a combined ambiguous scenario for PA-MUSIC by involving a large number of different partial arrays (*eg.* $n = 89$ in the above $\boldsymbol{d}_{55}$ example).

Nevertheless, if the majority of partial arrays share any particular manifold ambiguity, then the outlier probability can still be rather high, especially for low SNR's. This becomes evident if we consider the $m = 4$ source scenario for $\boldsymbol{d}_{55}$, where according to Table 1 there are only three partial arrays suitable for PA-MUSIC. These partial arrays have the following co-sequences:

$$\begin{aligned} \boldsymbol{c}_1 &= [3,\ 11,\ 4,\ 11] \\ \boldsymbol{c}_2 &= [3,\ 11,\ 4,\ 14] \\ \boldsymbol{c}_3 &= [3,\ 11,\ 15,\ 3]. \end{aligned} \tag{8}$$

Table 2 presents four example ambiguity generator sets [3] which are common to the above three partial arrays.

Each has an "ambiguity rank" [3] equal to four, meaning that any four DOA's from a set create the MUSIC pseudo-spectrum equivalent to the corresponding five-source scenario. The worst thing is that since these partial arrays only have five elements, the actual number of main MUSIC maxima is much greater than five, due to the sparsity of the partial arrays $\boldsymbol{c}_i$. (The order of the root-MUSIC polynomial for these partial arrays is equal to 29, 32 and 32 respectively.) For $\boldsymbol{c}_1$, the "ambiguity rank" is equal to three for ambiguity generator set 2. Thus if the signal scenario consists of $m = 3$ sources from this set, then this manifold ambiguity could be resolved by PA-MUSIC. Nevertheless for finite SNR, one could still expect a high abnormal trial probability.

Since the main purpose of PA-MUSIC is initialisation for some further maximum likelihood (ML) refinement procedure, its performance is measured here by the probability of abnormal trials. We first investigate a "super-resolution" scenario where the spatial frequencies of the $m = 3$ sources are set at $w \equiv \sin\theta =$

	$\sin\theta_1$	$\sin\theta_2$	$\sin\theta_3$	$\sin\theta_4$	$\sin\theta_5$
set 1	-1	0.4286	0.5714	0.7143	0.8571
set 2	-1	0.2727	0.4545	0.6364	0.8182
set 3	-1	0.5556	0.6667	0.7778	0.8889
set 4	-1	0.4667	0.6000	0.7333	0.8667

Table 2: Example ambiguity generator sets.

$[-0.5,\ 0,\ \Delta]$, where $\Delta = 0.05$. This signal scenario is far beyond the conventional beamwidth resolution limit for the 16-element ULA $\boldsymbol{d}_{15}$ of $w_{CBF} = 2/a = 0.133$. Inverting this relation, the ULA apertures required to resolve this separations by conventional beamforming is approximately $a_{crit} \simeq 2/0.05 = 40$. In [2] we demonstrated the improved DOA estimation accuracy of $\boldsymbol{d}_{55}$ over $\boldsymbol{d}_{15}$ using GSS. Here we concentrate on showing the reduction in abnormal DOA estimates using outlier mitigation after GSS.

Our experiment consists of 500 independent Monte-Carlo trials simulating independent realisations of single-snapshot stochastic data for $\boldsymbol{d}_{55}$. For comparison with the standard spatial smoothing approach, we also analysed the 16-element ULA $\boldsymbol{d}_{15}$ using forward and backward averaging of 14-element sub-arrays.

Fig. 2 presents the sample probability of abnormal trials for GSS (P_0) as a function of SNR (dash-dot line $\boldsymbol{d}_{15}$, dotted line $\boldsymbol{d}_{55}$). By the above CBF equation, almost all partial arrays under consideration have a beamwidth greater than the source separation $\Delta = 0.05$; only the $\boldsymbol{d}_{55}$ geometry has any partial arrays with aperture exceeding $a_{crit} \simeq 2/\Delta = 40$. Hence it is not surprising that for this close-source separation, both arrays have a high probability of abnormals, especially at low SNR's, but that $\boldsymbol{d}_{55}$ is the best initialiser. Indeed the probability of correct initialisation is, as we expect, directly related to the partial array aperture distribution, with $\boldsymbol{d}_{15}$ performing poorly. Fig. 2 also shows the two source scenarios $\Delta = 0.075$ and $\Delta = 0.1$ for comparison.

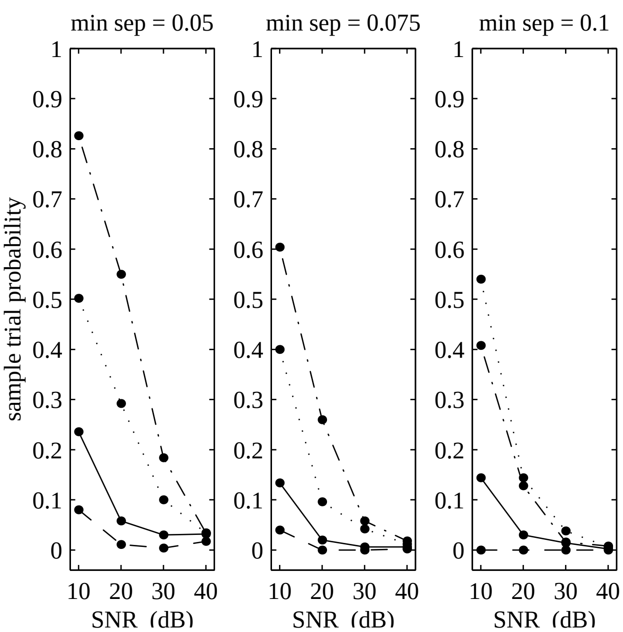

Figure 2: Abnormal trial probability for $\boldsymbol{d}_{55}$, with (P_1, solid line) and without (P_0, dotted line) outlier mitigation, for the probability P_2 (dashed line), and for $\boldsymbol{d}_{15}$ without outlier mitigation (dash-dot line).

2 OUTLIER MITIGATION ALGORITHM

When the number of fully correlated sources is rather small ($m \ll M$), we propose that the following local test be applied, where the full NLA snapshot is used. Let $\hat{\theta}_k^{(0)}$ ($k = 1, \ldots, m$) be the initial DOA estimates, obtained via the PA-MUSIC technique. We define the first iterate to be

$$\hat{\theta}_k^{(1)} = \arg\min_{\theta \in [-\frac{\pi}{2}, \frac{\pi}{2})} \boldsymbol{a}^H(\theta) \left[I_M - \frac{F_k^{(1)} \boldsymbol{y}\, \boldsymbol{y}^H F_k^{(1)}}{\boldsymbol{y}^H F_k^{(1)} \boldsymbol{y}} \right] \boldsymbol{a}(\theta) \tag{9}$$

where

$$\boldsymbol{a}(\theta) = \Big[1, \exp\left(i\pi d_2 \sin\theta\right), \ldots, \exp\left(i\pi d_M \sin\theta\right)\Big]^T , \tag{10}$$

$\boldsymbol{y} \in \mathcal{C}^{M\times 1}$ is the single vector of observed sensor outputs,

$$F_k^{(1)} = I_M - \tilde{A}_k^{(1)} \left(\tilde{A}_k^{(1)H} \tilde{A}_k^{(1)}\right)^{-1} \tilde{A}_k^{(1)} \tag{11}$$

and

$$\tilde{A}_k^{(1)} = \left[\boldsymbol{a}(\hat{\theta}_1^{(1)}),\ \ldots,\ \boldsymbol{a}(\hat{\theta}_{k-1}^{(1)}),\ \boldsymbol{a}(\hat{\theta}_{k+1}^{(0)}),\ \ldots,\ \boldsymbol{a}(\hat{\theta}_m^{(0)})\right]. \tag{12}$$

If now

$$\left|\hat{\theta}_k^{(0)} - \hat{\theta}_k^{(1)}\right| < \varepsilon \ll 1 \qquad \forall \quad k = 1, \ldots, m \tag{13}$$

then the initialising set of estimates $\hat{\theta}_k^{(0)}$ are passed on to the next stage of local ML refinement in the immediate neighbourhood of $\hat{\theta}_k^{(0)}$. The threshold tolerance value ε is defined by the expected accuracy, as determined by the appropriate Cramér-Rao bound. The exact choice of ε is not critical, since in most cases abnormal estimates are essentially randomly distributed.

If, however, at least one of the new estimates $\hat{\theta}_k^{(1)}$ differs significantly from its counterpart $\hat{\theta}_k^{(0)}$, then the set $\hat{\theta}_k^{(0)}$ is understood to contain one or more outliers. In this case the DOA set $\hat{\theta}_k^{(1)}$ can be iterated upon similarly to Eqn. (9). If the new estimates $\hat{\theta}_k^{(2)}$ satisfy the convergence condition of Eqn. (13) then the outlier(s) have been successfully removed, and the set $\hat{\theta}_k^{(2)}$ is passed on for ML refinement; otherwise we continue iterating up to some maximum number.

Thus in general, if the iterates $\hat{\theta}_k^{(\ell)}$ ($\ell = 0, 1, \ldots$) do not converge to some stable point satisfying Eqn. (13), the estimation trial is treated as unsuccessful; that is, the algorithm detected the presence of outlier(s), but could not correct the situation. If the iterates do converge, then the algorithm should have detected and corrected the outlier(s). If the first iterate is essentially identical to the zeroth iterate, then the algorithm confirms the non-existence of outliers.

The following example illustrates successful outlier mitigation in the array $\boldsymbol{d}_{55}$ for $w = [-0.5,\ 0,\ 0.05]$ and

ℓ	$\hat{\theta}_1^{(\ell)}$	$\hat{\theta}_2^{(\ell)}$	$\hat{\theta}_3^{(\ell)}$
0	-0.5054	0.9331	0.3540
1	-0.4994	-0.0027	0.0505
2	-0.4999	-0.0012	0.0510

Table 3: Convergence of example iterates $\hat{\theta}_k^{(\ell)}$ for $\boldsymbol{d}_{55}$.

30 dB SNR. Table 3 shows the progression of iterates $\hat{\theta}_k^{(\ell)}$ over the three sources for the NLA $\boldsymbol{d}_{55}$, where $\varepsilon = 0.01$. We see that the initial DOA estimate set contains two outliers, with a single reasonable $\hat{\theta}_1$ which is somewhat close to the true value. Even in this very difficult case, the proposed outlier mitigation algorithm demonstrates its ability to identify and to correct the outliers. Subsequent local ML refinement is effective in then increasing the DOA estimation accuracy close to the corresponding Cramér-Rao bound [2].

The solid line in Fig. 2 shows the overall abnormal trial probability after outlier mitigation (P_1) for the same simulation experiment. We see that P_1 is significantly less than the original probability P_0.

As well as simply comparing the new overall abnormal trial probability against the original probability, the efficiency of the proposed algorithm can be measured by its failure probabilities: the mis-identification of a normal initial DOA set $\hat{\theta}_k^{(0)}$ as abnormal (*ie.* diverging iterations or converging to a stable but incorrect DOA set, P_2); failing to correct abnormal trials (*ie.* converging incorrectly, P_3); and abnormal trials which are abnormally identified but uncorrectable (due to diverging iterations, P_4).

The dashed line in Fig. 2 shows the probability P_2 in our 500-trial experiment. Clearly mis-identification is very unlikely in this scenario. The other probabilities P_3 and P_4 are conditional upon initially abnormal trials; for moderate SNR, we encounter the asymptotic domain where the number of such trials become statistically not significant, so that rather than plotting these conditional probabilities, we merely mention that they were found to be around 15–35% and 0–10% respectively for the examined scenario.

Finally, to demonstrate the specific ability of our approach to resolve partial-array manifold ambiguity, we consider two $m = 4$ source scenarios.

In the first trial, we begin with the first four DOA's of the ambiguity set 1 from Table 2. Evaluation of the deterministic PA-MUSIC pseudo-spectrum then correctly locates three DOA's, with one outlier. Ten random trials of the outlier mitigation algorithm for this abnormal set and 40 dB SNR each resulted in the outlier being corrected.

In the second trial, we have chosen the "super-resolution" scenario

$$w = \{-1.000, 0.2727, 0.8182, 0.8572\} \qquad (14)$$

as a variation of ambiguity set 2 in Table 2. In this case, nine out of ten random trials were successfully able to identify and correct the outlier.

3 SUMMARY

We have introduced an outlier mitigation algorithm which significantly decreases the probability of abnormal trials for generalised spatial smoothing. The entire approach to DOA estimation for a small number of fully correlated sources (a problem arising, for example, with multimode signals from a single source, or bearing estimation and resolution of several radar targets that cannot be resolved in range nor Doppler) is then to apply PA-MUSIC followed by outlier mitigation, followed by ML local refinement. This overall procedure is a significant improvement on standard ULA and spatial smoothing (for a small number of fully correlated sources).

References

[1] T.J. Shan, M. Wax, and T. Kailath, "On spatial smoothing for direction-of-arrival estimation of coherent signals", *IEEE Trans. Acoust. Sp. Sig. Proc.*, vol. 33, pp. 806–811, 1985.

[2] Y.I. Abramovich and N.K. Spencer, "Generalised spatial smoothing using partial arrays for multiple target bearing estimation", in *Proc. ICASSP-98*, Seattle, 1998.

[3] C. Proukakis and A. Manikas, "Study of ambiguities of linear arrays", in *Proc. ICASSP-94*, Adelaide, 1994, vol. 4, pp. 549–552.

[4] Y.I. Abramovich, D.A. Gray, N.K. Spencer, and A.Y. Gorokhov, "Ambiguities in direction-of-arrival estimation for nonuniform linear antenna arrays", in *Proc. ISSPA-96*, Gold Coast, 1996, pp. 631–634.

[5] Y.I. Abramovich and N.K. Spencer, "Optimisation methods in nonuniform linear antenna array design and signal processing", in *Proc. ICOTA-98*, Perth, 1998.

[6] Y.I. Abramovich, D.A. Gray, A.Y. Gorokhov, and N.K. Spencer, "Positive-definite Toeplitz completion in DOA estimation for nonuniform linear antenna arrays — Part I: Fully-augmentable arrays", *IEEE Trans. Sig. Proc.*, submitted 1995, accepted 1998.

[7] N.K. Spencer, "Optimal partial-array design of nonuniform linear antenna arrays", In preparation.

[8] A. Flieller, P. Larzabal, and H. Clergeot, "Study of ambiguities in array manifold: A general framework", in *Proc. SSAP-96*, Corfu, 1996, pp. 574–577.